Characteristics of Dryline Passage during COPS-91

TODD M. CRAWFORD AND HOWARD B. BLUESTEIN

School of Meteorology, University of Oklahoma, Norman, Oklahoma

(Manuscript received 7 March 1996, in final form 29 July 1996)

ABSTRACT

The characteristics of dryline passage are documented through an analysis of data from an instrumented surface mesonetwork in the Texas panhandle, and western and central Oklahoma during the Cooperative Oklahoma Profiler Studies field program. Some eastward-moving drylines at the surface during the day were characterized by monotonic drops in dewpoint after dryline passage; others were marked by a *series* of rapid drops punctuated by periods of no change after dryline passage, which suggests that the dryline often progresses in *discrete steps*, rather than continuously. The dryline during the daytime was not always collocated with a pressure trough, although the strongest dryline observed was. Analyses of surface pressure traces indicated that westward-moving drylines during the evening did not display behavior characteristic of strong, intense density currents, as had been found in other studies. Evidence is presented, in one case, of 90-min oscillations in water vapor and wind behind the dryline, which may have been associated with the downward transport of momentum associated with gravity waves aloft.

1. Introduction

The dryline in the plains region of the United States is a low-level boundary separating moist, relatively cool maritime air that has passed over the Gulf of Mexico, from dry, relatively warm continental air that has flowed over the elevated terrain to the west (McGuire 1960); it is found most often during the spring. It is important not only because different weather conditions are found on either side of it but also because it is frequently the site of the initiation of convective storms (Rhea 1966), many of which become severe and produce damaging straight-line winds, tornadoes, and large hail (Bluestein and Parker 1993).

The dryline typically propagates to the east during the day and retreats to the west at night (Schaefer 1974a). Numerical simulations indicate that vertical mixing of momentum and water vapor, and the east–west variation in the depth of the moist boundary layer east of the Rockies, play important roles in the eastward motion of the dryline (Schaefer 1974b; Sun and Wu 1992; Ziegler et al. 1995). In some cases the airflow in westward-moving drylines behaves like a density current (Fujita 1970; Parsons et al. 1991; Ziegler and Hane 1993; Ziegler et al. 1995) in that ''heavy'' air of relatively low virtual temperature east of the dryline displaces ''light'' air of relatively high virtual temperature west of the dryline: the light air mass flows up and over the low-level heavy air mass.

Our knowledge of the observed structure of the dryline is based upon synoptic-scale surface and upper-air observations (e.g., Bluestein et al. 1988), aircraft data (Fujita 1958; McGuire 1960; Hane et al. 1993), special soundings (e.g., McCarthy and Koch 1982), and numerical simulations (Schaefer 1974b; Sun and Wu 1992; Ziegler et al. 1995). The dryline during the daytime appears to be nearly vertically oriented, with a deep, well-mixed, dry boundary layer to the west and a moist boundary layer to the east, which is capped by potentially warm, dry air aloft. Although the defining characteristic of a dryline is a zone of strong gradient in water vapor content, a shift in wind direction along or near the dryline is often also found, and synoptic maps usually show a pressure trough analyzed along the dryline.

However, the *mesoscale* nature of the dryline makes it unamenable to observational study using only data from the standard observing network. Observations of the dryline on the mesoscale and on shorter (e.g., convective) scales require nonstandard instrumentation and/or platforms such as aircraft, special or mobile soundings, and surface mesonetworks. Of the studies based upon data from special instruments (Beebe 1958; Fujita 1958; McGuire 1960; NSSP Staff 1963; Koch 1979; McCarthy and Koch 1982; Koch and McCarthy 1982; Sanders and Blanchard 1993; Ziegler and Hane 1993; Hane et al. 1993) only a few have provided documentation of the time-dependent behavior of the dryline at the surface. Some of these studies have suggested the

Corresponding author address: Todd M. Crawford, School of Meteorology, University of Oklahoma, 100 E. Boyd, Rm. 1310, Norman, OK 73019.
E-mail: tcrawf@rossby.metr.ou.edu

possible dynamical importance of density gradients directed across the dryline. Since both temperature and dewpoint contribute to density, and a dryline is characterized by the dewpoint gradient and change in wind across it, the cross-dryline component of the virtual temperature gradient, the pressure gradient, and the wind are of interest.

During the Cooperative Oklahoma Profiler Studies field program in May 1991 (COPS-91), the structure and behavior of the dryline were documented using an automated mesoscale network of surface stations, aircraft traverses across the dryline, and special soundings (Hane et al. 1993). The purpose of this paper is to use COPS-91 data to document the nature of dryline passages at the surface, on the convective and mesoscale timescales, that is, on timescales of minutes to hours.

In particular, we seek answers, which are based on observations during COPS-91, to the following questions:

1) How is the nature of eastward-moving drylines different from the nature of westward-moving drylines?
2) Do density current dynamics play a role?
3) What is the variety of behavior that is observed?

In this study we focus on dryline structure near the surface but do not address the issue of the initiation of cumulus convection, which is discussed elsewhere (e.g., Ziegler et al. 1994a; Hane et al. 1997), or the detailed three-dimensional structure of the dryline determined from analyses of aircraft data, a study of which is in progress and will be discussed elsewhere also. In section 2 we detail the nature of the data and the processing procedures we used. The nature of both eastward- and westward-moving drylines is discussed in section 3. A summary of the results of our study, conclusions, and suggestions for continued work are found in section 4.

2. Data and data processing

The network of surface observing sites during COPS-91 is shown in Fig. 1. Eight sites of the fifteen Portable Automated Mesonetwork-II (PAM-II) (Brock et al. 1986) stations from the National Center for Atmospheric Research (NCAR) were chosen to fill in the gaps between neighboring standard hourly surface observation sites; seven stations were located in a finer-scale grid in central Oklahoma for other studies. At each site, 60-s averages of station pressure, dry-bulb temperature, relative humidity, water vapor mixing ratio, and the zonal (u) and meridional (v) components of the wind were available every 60 s. Calculations of monthly averages of each variable were used to determine and remove biases subjectively and to discard apparently erroneous data. Missing data were estimated through temporal linear interpolation. Overall, 6.3% of all the PAM-II data were missing. Of these, most occurred at Quitaque, where approximately two-thirds of the data (representing approximately 20 days) were not available, and at McLean, where approximately one-third of the data were missing. In the few instances in which interpolated data were used, the longest time interval over which data were interpolated was less than an hour. Interpolated data were not used to support any of our findings.

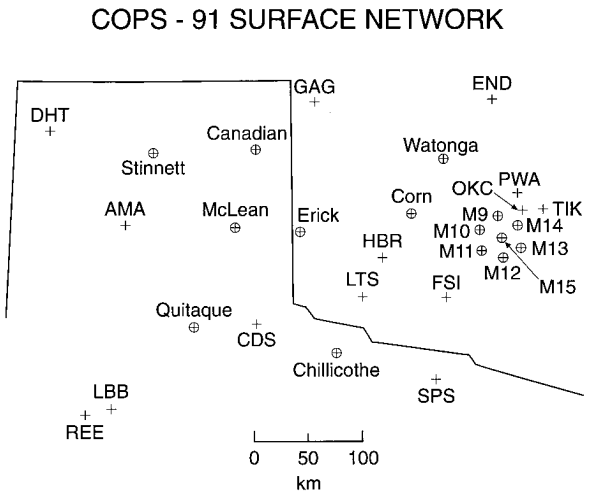

FIG. 1. Distribution of surface observing sites during COPS-91. PAM-II sites are represented by circles with inscribed crosses; standard hourly surface observing sites are represented by crosses.

A time series of station pressure was produced in which the diurnal and semidiurnal oscillations (Simpson 1918; Haurwitz 1955; Chapman and Lindzen 1970, 4–21), due mainly to the diurnal variation in surface temperature and heating from the absorption of radiation by water vapor and ozone, were removed. The nature and magnitude of the oscillations were determined through Fourier analyses of the 60-s pressure data at each PAM-II site for the entire month of May. The spectra (not shown) exhibited well-defined peaks at 12 and 24 h, and also at periods of 4 and 10.5 days, the latter two of which represent the passage of synoptic-scale systems through the PAM-II network. The diurnal and semidiurnal pressure oscillations averaged over all PAM-II sites are shown in Fig. 2. The combined oscillations have an amplitude of approximately 1.6 mb, which is only slightly greater than the 1.4-mb amplitude found from a 10-yr average (1931–40) at Amarillo, Texas, during May (U.S. Department of Commerce 1943).

3. Documentation of dryline passages

Surface maps and time series of data from PAM-II stations were used to infer the convective-scale features of the dryline at the surface. The PAM-II data were not temporally filtered, so that the maximum possible time resolution could be attained.

Just as the passage of a cold (warm) front is marked by a decrease (increase) in temperature, the eastward (westward) passage of a dryline is marked by a decrease (increase) in water vapor, represented by the dewpoint

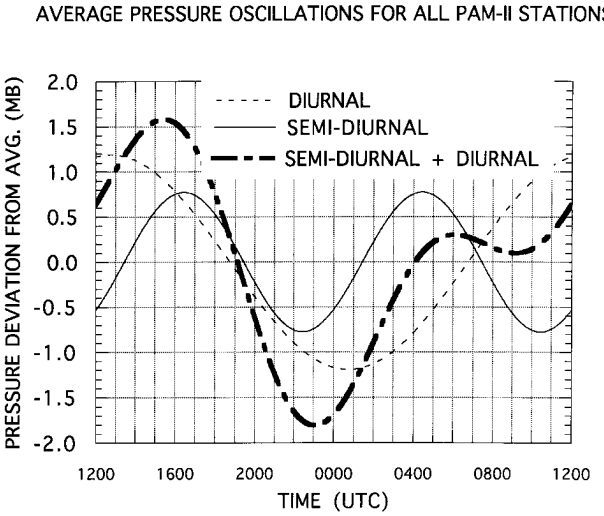

FIG. 2. Deviation of station pressure (from its May 1991 average) as a function of time of day (thick dashed–dotted line) averaged at all PAM-II sites (cf. Fig. 1). Diurnal (semidiurnal) component is represented by thin dashed (thin solid) line.

temperature. Based subjectively on the inspection of many analyses of drylines, we define the criterion for eastward (westward) dryline passage to be a decrease (increase) in dewpoint of at least 3°C (2°C) at a rate of at least 0.5°C h^{-1}. Temporal and spatial continuity (or lack thereof) of dryline passage at neighboring stations confirms (or casts doubt) that a dryline has actually passed. Oscillations in dewpoint related to waves along the dryline (Koch 1979; Sanders and Blanchard 1993) and outflow from convective activity (Bluestein et al. 1988, 1989) may mask dryline passage.

Based upon analyses of the COPS-91 mesonet data and standard surface data at hourly intervals during May 1991, there were 7 (6) days in which an eastward-moving (westward moving) dryline passed by one or more stations in the PAM-II network. Instances in which drylines moved eastward past PAM-II stations occurred between 0840 and 1915 CDT; instances in which drylines moved westward past PAM-II stations occurred between 1600 and 2200 CDT. As has been noted by Schaefer (1974a), eastward-moving drylines generally occur during the day, while westward-moving drylines occur during the late afternoon or evening. Fourteen (twelve) eastward-moving (westward moving) dryline passages were documented at operational PAM-II stations. Since the dryline often passed more than one PAM-II station on a given day, there are more dryline passages than dryline days. However, on any given dryline day there were an average of only two dryline passages, that is, only two stations experienced dryline passage. This implies that the dryline generally moved no farther east than the westernmost portion of the PAM-II network throughout the month. A representative selection of traces of dewpoint temperature, wind, pressure, and virtual temperature are now examined to see if there are systematic relationships among them while a dryline is passing by the sites. Traces examined do not include linearly interpolated missing data.

a. Eastward-moving drylines

1) 30–31 MAY

The location of the dryline in the Texas panhandle at midday on 30 May is indicated in Fig. 3a. In this and subsequent maps, the dryline is analyzed along a zone in which the horizontal dewpoint gradient is on the order of 10°C $(100\ km)^{-1}$ or greater. During the afternoon the dryline remained quasistationary (Fig. 3b) and by 0300 UTC (all times henceforth given in UTC; CDT is 5 h earlier) had progressed eastward past Quitaque, Texas, in the southern section of the panhandle but had retreated westward past Stinnett, Texas, (Figs. 3c,d) in the northern portion of the panhandle. Figure 4 depicts a well-defined dryline passage at Quitaque at approximately 0010 31 May. The drop in surface dewpoint of 17°C in less than 15 min is accompanied by a shift in wind direction from southeasterly to southwesterly (Fig. 4a) and the beginning of a significant decrease in virtual temperature (Fig. 4b). The relatively weak response of the virtual temperature to the drastic dewpoint drop can be explained by the 1.5°C increase in temperature that accompanied dryline passage. The lowest ''adjusted'' pressure (i.e., the actual station pressure less the contribution from the diurnal and semidiurnal oscillations) occurred approximately the same time as dryline passage (Fig. 4b).

Satellite imagery indicates that a line segment of convective storms formed around 2000 (not shown) just east of the dryline, but radar observations show that the storms had weakened considerably or had dissipated by 2300; no severe weather was reported with these storms. Severe convective activity, however, did occur to the northeast in extreme western Oklahoma. There was no convective activity in the vicinity of Quitaque at the time of dryline passage.

After the dryline had passed, there were 90-min oscillations in dewpoint and wind direction for about 6 h, until 0600 (but not after 0600; traces are not shown after 0600): backing (veering) of the wind was accompanied by an increase (decrease) in dewpoint (Fig. 4a). Figure 4c clearly shows oscillations in the zonal component of the wind of approximately 2 m s^{-1} in amplitude, after the dryline passage, which was marked by a rapid shift from around -5 m s^{-1} to $+4$ m s^{-1} after 0000. The oscillations were not apparent at any other PAM-II site. No sites were available upstream (with respect to the upper-level flow), and hence the oscillations could not be tracked from one station to another. Oscillations near the dryline, of dewpoint and wind direction having periods of 17 and 140 min, have been noted by Koch (1979), and by Davies-Jones and Zacharias (1988) and Sanders and Blanchard (1993), respectively. However,

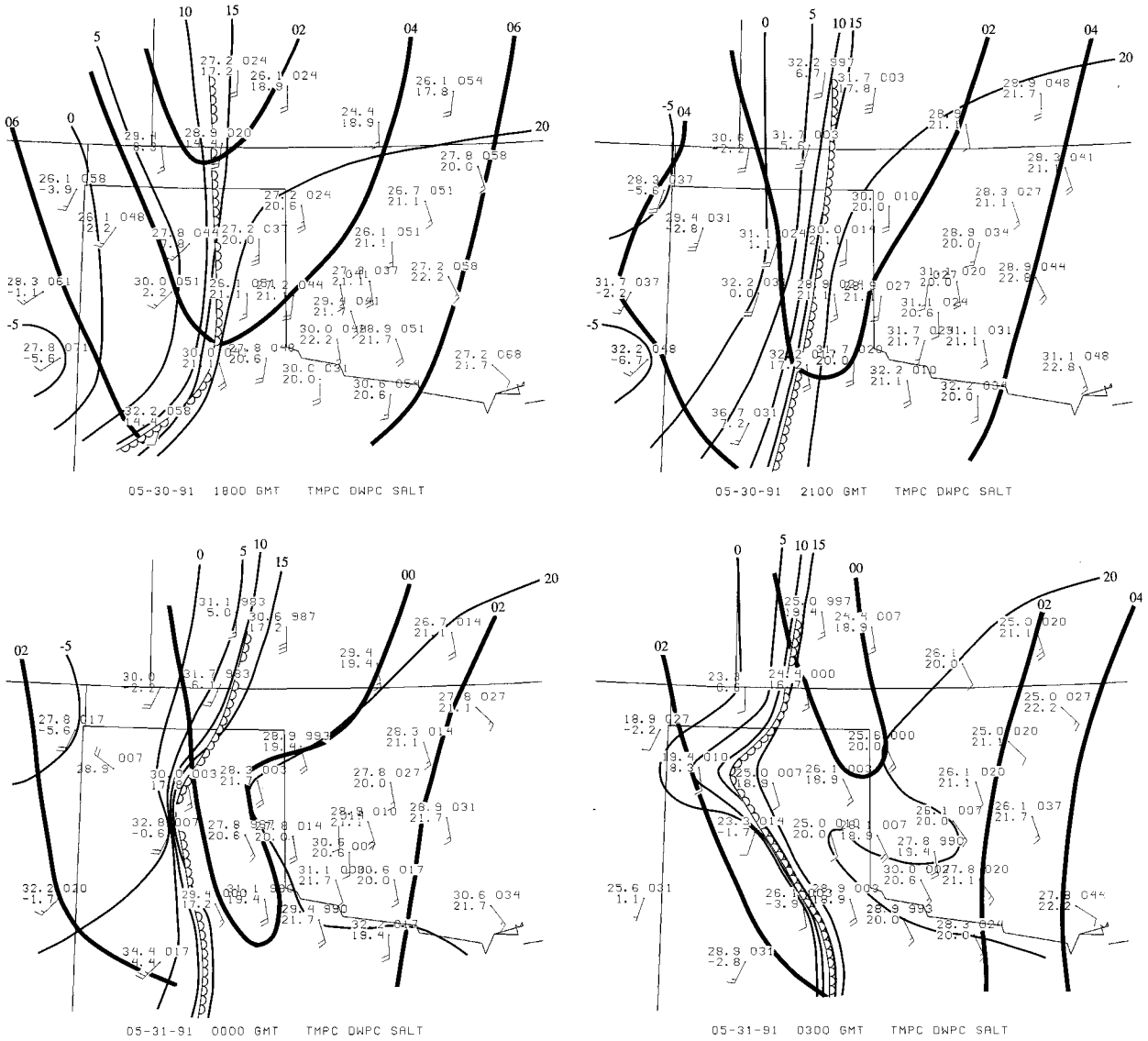

FIG. 3. Surface map for the COPS-91 region of western Oklahoma, the Texas panhandle, and adjacent areas at (a) 1800, (b) 2100, (c) 0000, and (d) 0300 UTC 30 (31) May 1991. Location of the dryline is denoted by the scalloped line. Temperature (upper left) and dewpoint (lower left) are plotted in degrees Celsius; altimeter setting in millibars times 10, without the leading ''10,'' is plotted to the right [the altimeter setting plotted at Chillicothe (cf. Fig. 1) is approximately 1.5 mb too low]; half (whole) wind barb represents 2.5 (5) m s^{-1}. Subjective analysis of altimeter setting isobars (thick solid contours) is in millibars times 10, without the leading ''10,'' and isodrosotherms (thin solid contours) in degrees Celsius.

corresponding oscillations in adjusted station pressure with amplitudes in excess of 0.1 mb were *not* apparent (Fig. 4b), possibly due to the 0.4-mb inaccuracy associated with the PAM-II sensors. Hour-scale oscillations in virtual temperature having amplitudes of approximately 0.7°C were superimposed on the diurnal decrease in virtual temperature: relative minima in virtual temperature were correlated with maxima in dewpoint for several hours (cf. Figs. 4a and 4b).

Satellite water vapor imagery, which depicts the amount of upper-tropospheric moisture, shows a band of enhanced moisture that extended from the Pacific Ocean into Arizona and most of New Mexico (Fig. 5a). A cusp located in southwestern New Mexico in the morning (not shown) had sharpened up and progressed into southeastern New Mexico by afternoon, and into the region just southwest of the COPS-91 area by early evening (Fig. 5b). Between 2100 and 0000 (but especially well portrayed at 2300) meridionally oriented bands (i.e., approximately transverse to the upper-level flow) in the water vapor imagery were visible just east of the cusp, several hundred kilometers or more southwest of Quitaque. In Fig. 5b there are several distinct bands near and just west of Lubbock in far western

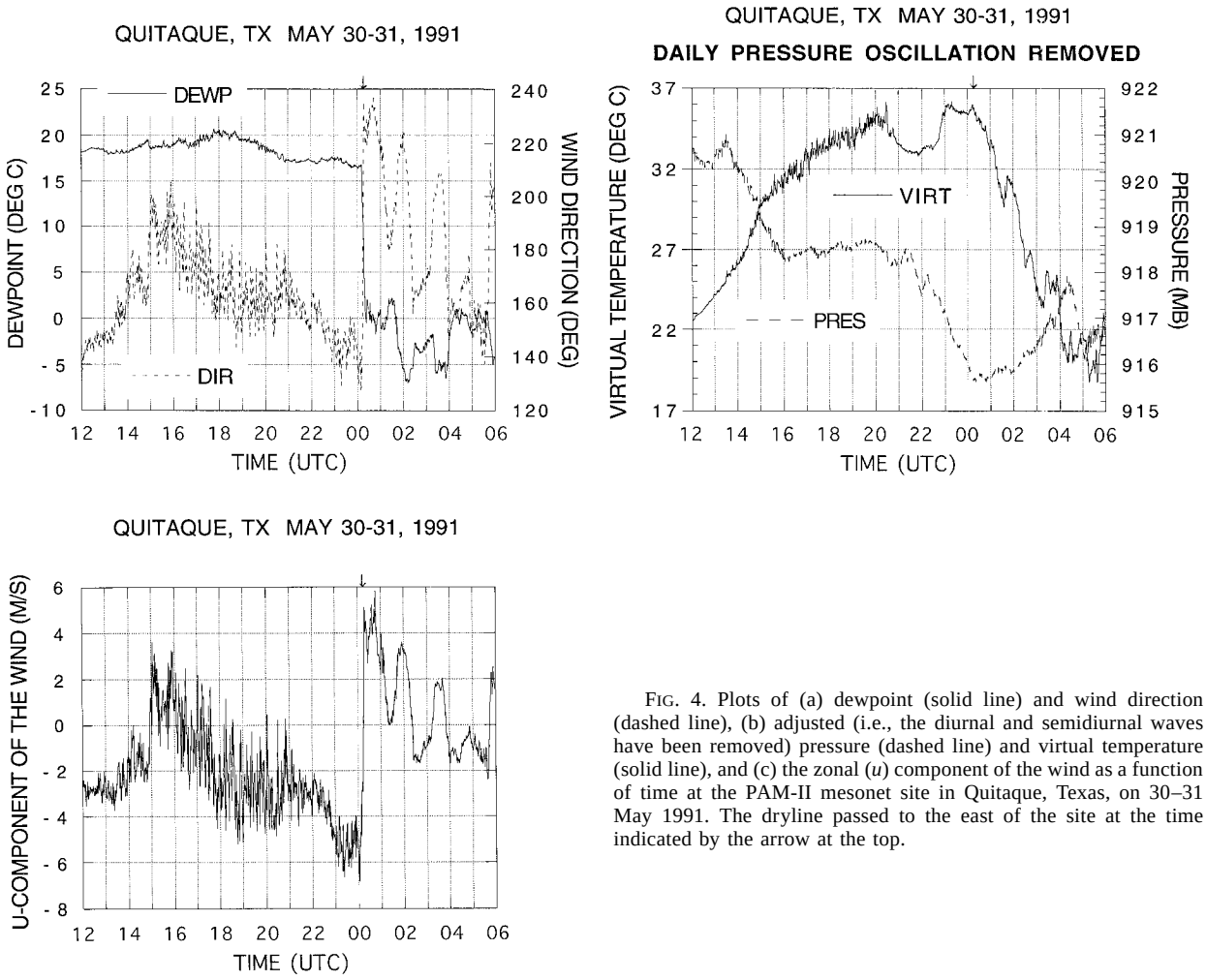

FIG. 4. Plots of (a) dewpoint (solid line) and wind direction (dashed line), (b) adjusted (i.e., the diurnal and semidiurnal waves have been removed) pressure (dashed line) and virtual temperature (solid line), and (c) the zonal (u) component of the wind as a function of time at the PAM-II mesonet site in Quitaque, Texas, on 30–31 May 1991. The dryline passed to the east of the site at the time indicated by the arrow at the top.

Texas. The bands, however, were not apparent after 0000 when the surface oscillations in dewpoint, etc. were apparent at Quitaque. The bands were approximately 40–50 km apart; a 90-min oscillation is consistent with an advective wave speed of 7–9 m s^{-1}, which is approximately identical to the zonal component of the 0000 31 May wind at 300 and 200 mb at nearby Midland, Texas (Fig. 6), but slower than that (12 m s^{-1}) at other nearby rawinsonde stations (Fig. 7). There is therefore some circumstantial evidence that there may have been a relationship between localized upper-tropospheric wave activity and surface oscillations behind the dryline; the amplitude of waves in the upper troposphere may have diminished after 0000 to the extent that they were no longer manifest in the water vapor imagery. Just to the southwest of Quitaque, the surface winds at Lubbock (LBB) and Reese Air Force Base (REE), which were from the south-southwest at only 2.5–5 m s^{-1} at 1800 (Fig. 3a), had picked up to 10 m s^{-1}, with gusts to 12 m s^{-1} from the west-southwest by 0000 (Fig. 3c). The maximum westerly wind component at LBB peaked at 0000 (Fig. 8). The atmosphere west of the dryline was well mixed below 600 mb (Fig. 6), and the strongest winds were found at relatively low levels, near 500 mb. The relatively late occurrence of maximum surface wind speed and the evidence from the water vapor imagery suggest that the wind shift and increase in speed at LBB was likely due to the downward vertical mixing of momentum (McCarthy and Koch 1982) associated with both dryline passage and oscillations associated with the aforementioned upper-tropospheric waves.

The character of dryline passage on the same day at Stinnett, Texas, in the northern Texas panhandle (Fig. 9) was quite different from that to the south at Quitaque. The dewpoint fell about 4°–7°C in four separate 15–30-min periods beginning just after 1600, while remaining approximately constant in between the falling periods (Fig. 9a). This steplike appearance in dewpoint trace was not evident in adjusted pressure or virtual temperature (Fig. 9b). However, it should be noted here that virtual temperature is much less sensitive to changes in dewpoint than to changes in temperature. Conversely,

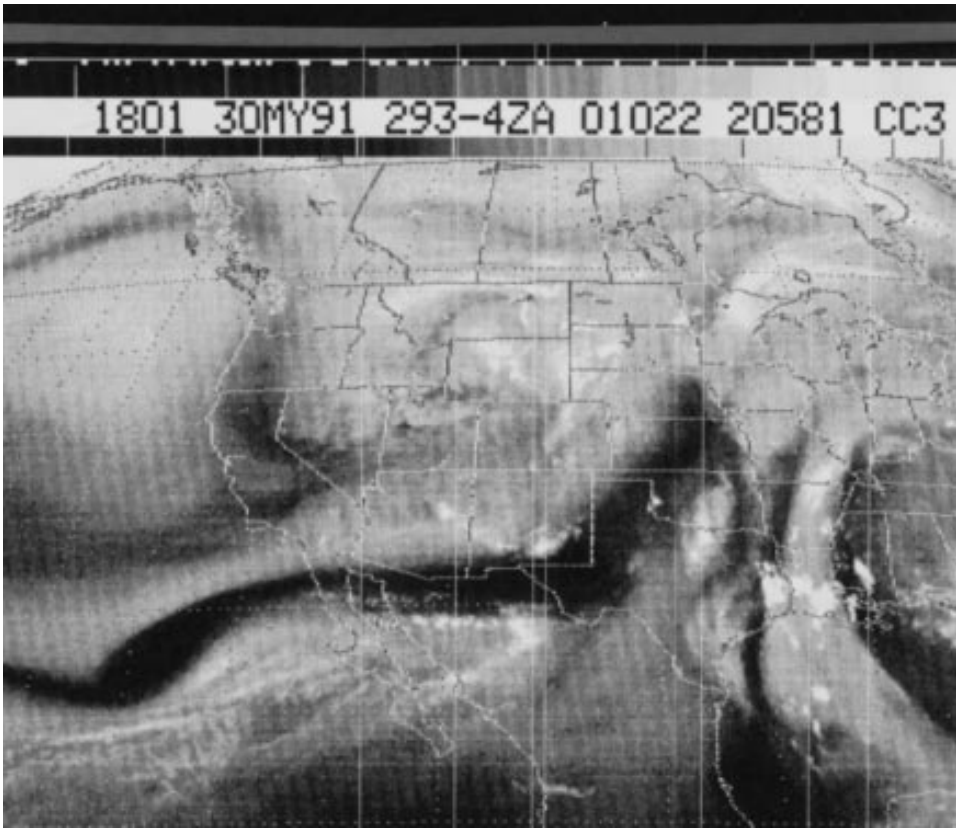

FIG. 5. Satellite imagery in the water vapor channel on 30 May 1991 at (a) 1801 and (b) 2301 UTC. The three meridionally oriented bands mentioned in the text are indicated by arrows on the image.

there was a correlation between dewpoint drop and wind direction. This is most evident in a plot of the *u*-component of the wind (Fig. 9c). The four periods during which the dewpoint fell began at approximately 1615, 1735, 1955, and 2120. It is clear that the *u*-component of the wind increases concurrently with the onset of the dewpoint drops. Similar steplike changes of water vapor across the dryline have been documented elsewhere and will be discussed in more detail in section 4 of this paper. The adjusted pressure was at a broad (about 2 h) relative minimum around the time of dryline passage just after 1600. The rate of virtual temperature rise decreased after dryline passage.

2) 26–27 MAY

Similar steplike traces of dewpoint were also apparent at McLean in the Texas panhandle during and after eastward dryline passage on 26 May. The location of the dryline in the Texas panhandle at midmorning is not apparent in Fig. 10a; dewpoints decrease gradually from east to west across the domain, with slightly more pronounced drying in eastern New Mexico. A pressure trough extends southward from a low pressure area in extreme northwest Oklahoma through western Oklahoma. At 1800 the dryline *is* apparent in the far western portion of the Texas panhandle (Fig. 10b). At this time, the dryline is not collocated with the pressure trough. The dewpoint at McLean dropped 5°C in about 30 min beginning just after 1500, followed by a 2.5°C rise in the next 30 min; it remained nearly constant from about 1600 until 1800 and then slowly dropped 6°C until 2030; just after 2200 it dropped a few more degrees Celsius (Fig. 11a). The dewpoint trace at Canadian, Texas, in the northern Texas panhandle was similar to that at McLean, except that the dewpoint continued to drop another 5°C after 2100 (Fig. 11a). This localized dewpoint drop resulted from a small area of drier air advecting in from the southwest, as detected by the NOAA P-3 aircraft (Hane et al. 1997). The location of the dryline was best defined in mid- to late afternoon (Figs. 10c,d) after it had appeared to jump eastward to a location approximately 100 km west of the pressure trough. There was no pressure mininum at McLean at the time the dewpoint had begun to drop after 1500 (Fig. 11b); instead, the adjusted pressure reached a minimum much later at 0000, about an hour or more after the time of minimum dewpoint (Fig. 11a). There was, however, a broad relative minimum in adjusted pressure at Canadian *after* the dewpoint had initially begun to fall (Fig. 11b). It therefore is likely that a surface pressure trough was not located within 100

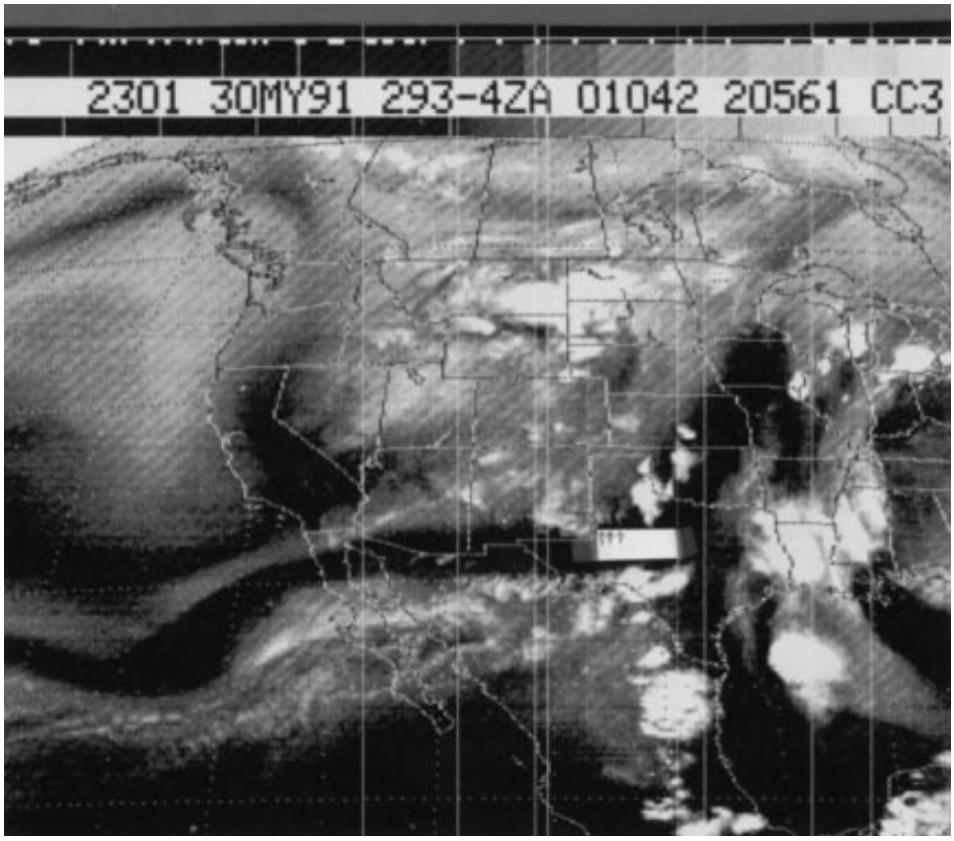

FIG. 5. *(Continued)*

km of the dryline until late in the afternoon and that the dryline moved eastward in discrete jumps, while the pressure trough moved slowly westward in response to the strong pressure falls occurring in the eastern Texas panhandle.

Tornadic storms occurred to the east and northwest about 0000, near the time of overall minimum adjusted pressure (Dowell et al. 1997). The wind directions at both McLean and Canadian (Fig. 11c) remained relatively constant from the south-southwest during the afternoon; however, the wind at Canadian veered more (i.e., was more westerly) than the wind at McLean. The virtual temperature traces at McLean and Canadian were similar (Fig. 11d); virtual temperature reached a broad maximum around 2100–2200. However, the virtual temperature jumped about 1°C at McLean when the dewpoint first dropped just after 1500 (cf. Fig. 11a) due to the warmer temperatures behind the dryline.

3) 12 MAY

The location of the dryline during late afternoon on 12 May is indicated in Fig. 12. The dryline passage at Stinnett in the northern Texas panhandle exhibited a relatively slow monotonic drop in dewpoint (Fig. 13a) beginning just before 1700 and continuing on until about 2030, by which time the dewpoint had dropped nearly 25°C. The wind was veering *before* the dewpoint had begun to drop and remained nearly constant in direction while the dewpoint was dropping. The dryline passage at Stinnett was more of a gradual process than an event. There was a relative minimum in adjusted pressure around 1900, 2 h after dryline passage (Fig. 13b). The trace of virtual temperature exhibited a broad maximum around 2300 (Fig. 13b), typical of the diurnal cycle for mid-May. On this day no convective activity occurred along or near the dryline.

b. Westward-moving drylines

1) 30 MAY

The retreat of the dryline westward past Stinnett on 30 May is documented in Figs. 9 and 3b–d. The dewpoint at 2330 jumped nearly 19°C in 5 min, while the wind direction backed from south-southwesterly to south-southeasterly (Fig. 9a), and the zonal component of the wind changed abruptly from around $+4$ to -3 m s^{-1} (Fig. 9c). The virtual temperature dropped suddenly about 1°C and then continued to drop off slowly at a constant rate; the adjusted pressure was unaffected and continued to fall, and reached a minimum over 3 h

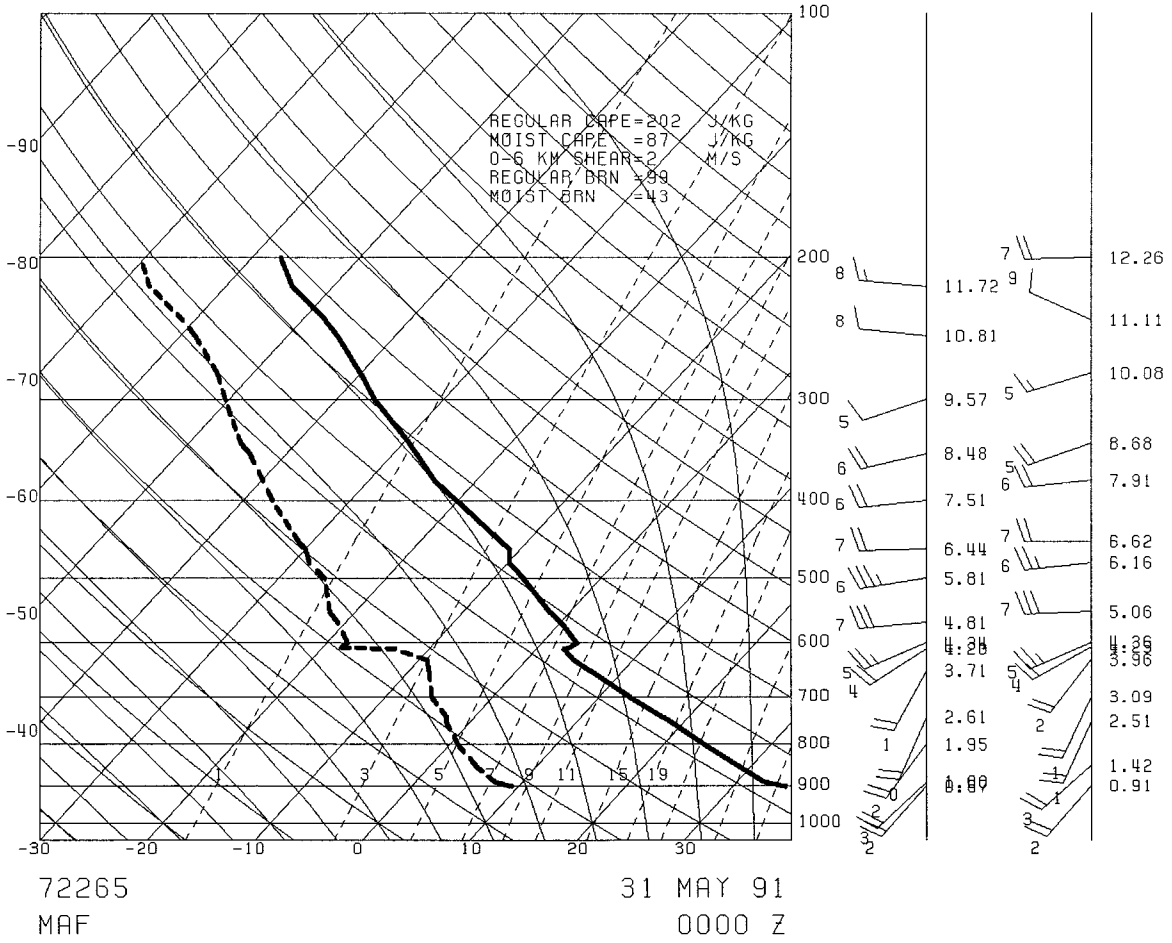

FIG. 6. Sounding (skew *T*–log*p* diagram) at Midland, Texas, at 0000 UTC 31 May 1991. Skewed abscissa is temperature (°C); ordinate is pressure (mb). Temperature (°C, solid contour); dewpoint (°C, dashed contour); half and whole wind barbs (at right) represent 2.5 and 5 m s^{-1}, respectively; tens unit of wind direction plotted at end of each wind barb. Height above sea level (km) plotted by each wind barb.

after the dryline had passed by the mesonet site (Fig. 9b). The sudden virtual temperature drop of 1°C was less than that which typically accompanies gust fronts (i.e., 5°–10°C); therefore, in the absence of large temperature changes aloft, one would not expect the surface pressure to change hydrostatically as much as it does when a gust front passes. However, Simpson (1969) documented sea-breeze cases with 1°C drops and pressure rises of a few tenths of a millibar. The pressure in this case was unaffected. This lack of any pressure response at all creates doubt as to whether this retreating dryline was acting as a density current. It is quite possible that the moisture return was so shallow that the hydrostatic pressure response was minimal. After the dryline had retreated the amplitude of the minute-scale fluctuations in virtual temperature was reduced considerably, probably a result of a decrease in turbulent motion due to the reduced vertical scale of turbulent eddies in the more shallow boundary layer east of the dryline.

2) 26–27 MAY

The character of the retreat of the dryline on 26–27 May past McLean and Canadian is shown in Fig. 11. Although the dewpoint (Fig. 11a) rose rapidly first at Canadian just before 0000, and later at 0300 at McLean, the adjusted pressure (Fig. 11b) traces at both sites were similar; the pressure began to rise around 0000, which at McLean was 3 h before the dryline actually had passed by. This lends credence to the hypothesis that the dryline is not always collocated with the pressure trough. However, the pressure changes, which were gradual, were only around a millibar or less over a 1-h time period. This is not similar to the sharper pressure changes that occur when a gust front passes by. The wind direction (Fig. 11c) at McLean backed around 2315 from south-southwesterly to southerly, with an accompanying rise in dewpoint of several degrees Celsius. The wind further backed just after 0200, and almost an hour later was followed by a relatively slow mono-

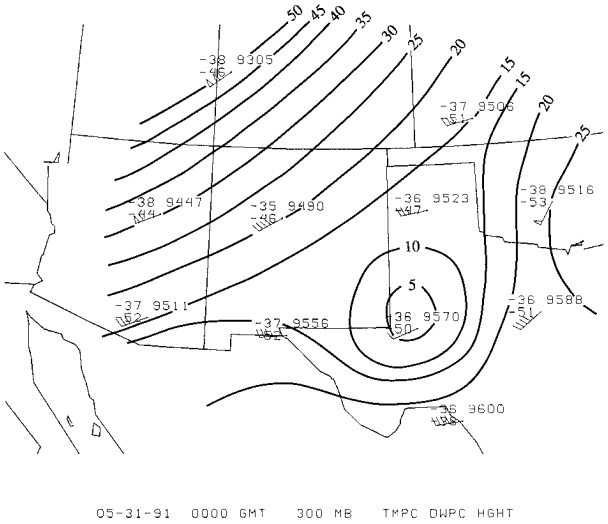

FIG. 7. Isotach analysis (m s^{-1}, solid) at 300 mb at 0000 UTC 31 May 1991. Temperature and dewpoint plotted in degrees Celsius; 300-mb height plotted in meters. Half, whole, and flagged wind barbs represent 2.5, 5, and 25 m s^{-1}, respectively.

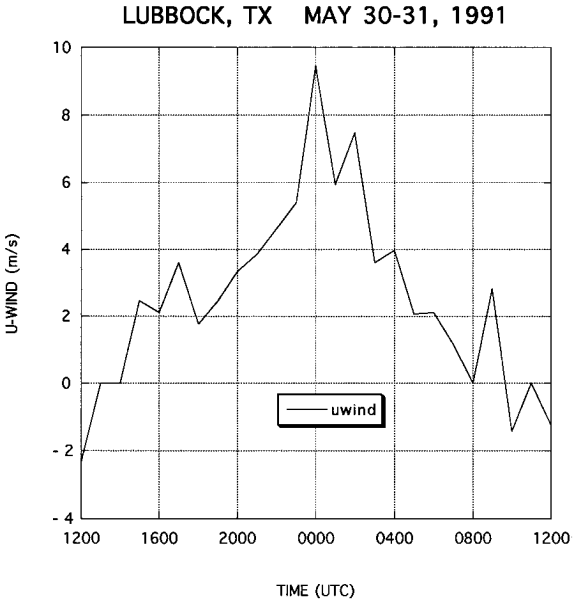

FIG. 8. Zonal (u) component of the wind at Lubbock, Texas, from 1200 UTC 30 May 1991 to 1200 UTC 31 May 1991.

tonic rise in dewpoint. At McLean the westward dryline passage was therefore not abrupt. Although at Canadian the wind backed abruptly around 0130 from southwesterly to southerly or south-southeasterly, the dewpoint had begun to rise over an hour earlier. The drop in virtual temperature that had begun around 2300 was halted abruptly around 0130 (Fig. 11d). At McLean the virtual temperature began to fall again around 0300, which is coincident with the time the dewpoint had begun to rise. The westward dryline passages at McLean and Canadian therefore were not marked by *simultaneous* (i.e., on a timescale of minutes) backing of the wind, drop in virtual temperature, and rise in pressure. A qualitative examination of some westward dryline passages using data from the recent Oklahoma Mesonet (Brock et al. 1995) has confirmed these nonclassic results.

3) 12–13 MAY

At Stinnett on 12–13 May (Fig. 13) the westward dryline passage was relatively complex. Although the dewpoint had begun to rise around 2230 while the wind backed slightly, the dewpoint abruptly dropped again around 0030 as the wind veered (Fig. 13a); the adjusted pressure during this period fell slowly and steadily (Fig. 13b). The dewpoint rose rapidly again around 0130, while the wind backed (Fig. 13a). The wind direction [and zonal component of the wind (Fig. 13c)] subsequently underwent several periodic steplike changes at approximately 2-h intervals, while the dewpoint rose in a steplike fashion: during the periods of rapid dewpoint rise just after 0130 and again around 0330, there were approximately 10-min periods of sharply backed winds and increases in the easterly wind component of the wind of around 4 m s^{-1}. Changes in adjusted pressure (Fig. 13b) were less than 1 mb and were not well correlated with the changes in the other variables. The virtual temperature began to decrease rapidly an hour before the dryline had actually passed by, owing to the diurnal reduction in heating.

4. The ''stepped'' nature of drylines

Three of the five eastward-moving dryline cases in this study exhibited steplike changes of water vapor. Ziegler and Hane (1993) were the first to document this steplike behavior, through an examination of the surface data recorded by an instrumented, moving vehicle during the Central Oklahoma P-3 Studies field program (COPS-89). During the 24 May 1989 dryline case, the time series of water vapor mixing ratio was composed of two steps, similar to the dryline passage at McLean on 26 May 1991 [cf. Fig. 11a with Fig. 7a from Ziegler and Hane (1993)]. They found, using saturation-point analysis (Betts 1982), that the extra step was representative of a third airmass type, composed of a mixture of volumes of air originating from either side of the dryline. This region was logically termed the ''mixing zone'' and was approximately 10 km in width. Approximately 100 min after the documentation of the two-stepped dryline, a National Oceanic and Atmospheric Administration P-3 aircraft detected three steps in a traverse across the dryline at 150–300 m AGL (Fig. 8a; Ziegler and Hane 1993). This time series is comparable to those at Stinnett on 30 May 1991 (Fig. 9a) and Canadian on 26 May 1991 (Fig. 11a). Hane et al. (1993), in a review of the COPS-91 dryline cases, noted the existence of multiple dewpoint gradients on four sep-

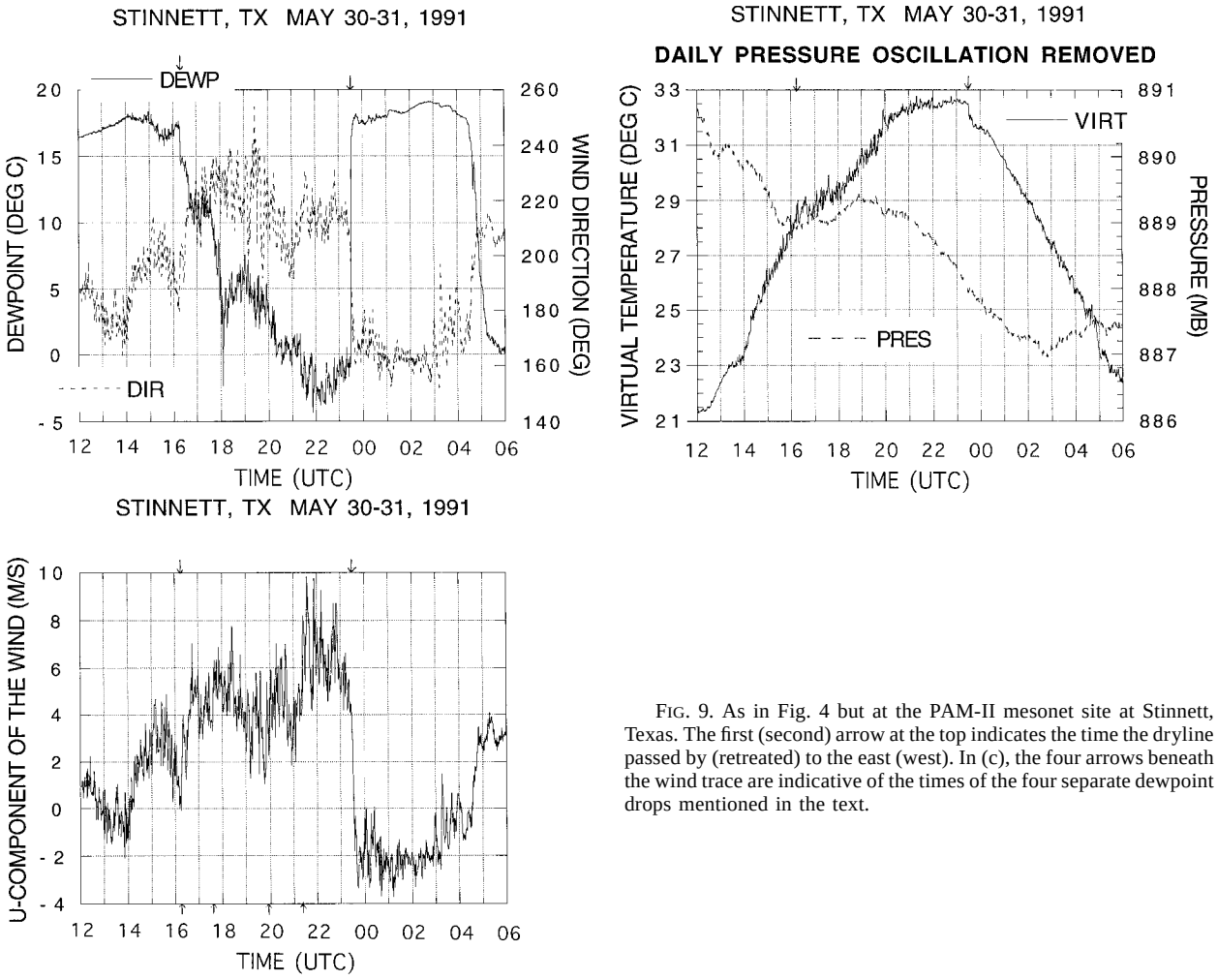

FIG. 9. As in Fig. 4 but at the PAM-II mesonet site at Stinnett, Texas. The first (second) arrow at the top indicates the time the dryline passed by (retreated) to the east (west). In (c), the four arrows beneath the wind trace are indicative of the times of the four separate dewpoint drops mentioned in the text.

arate days. They speculated that compensating downdrafts to the east of the updrafts at the dryline would act to warm and dry the boundary layer there, resulting in a second moisture gradient just to the east of these downdrafts. Ziegler et al. (1995) noted that these ''microfronts'' were reflective of the local state of mixing at the dryline and may be similar to the ''mesoscale moisture fronts'' described by Mahrt (1991). Shaw et al. (1997) were able to numerically simulate a double moisture gradient at the dryline and suggested that it may be caused by a breakdown of a simple vertical circulation east of the dryline into multiple circulations. Hane et al. (1997) were able to show that both single and double moisture gradients could exist concurrently along the same dryline.

The instrumentation used in the COPS-91 project was not designed to measure turbulent characteristics of the boundary layer accurately (C. Ziegler 1995, personal communication). However, during the Hydrological and Atmospheric Pilot Experiment (André et al. 1986) there was a more rigorous emphasis on the accurate measurement of turbulent moisture fluctuations in the boundary layer. During two particular flights over a relatively homogeneous pine forest on days with little surface evaporation and with dry air above the boundary layer, coherent moisture variations on the scale of 10 km were documented (Fig. 2; Mahrt 1991). In this type of boundary layer, pockets of dry air are able to mix turbulently to the surface and produce local moisture gradients. These 10-km variations were sometimes also associated with strongly convergent zones of width 1 km or smaller. These ''moisture fronts'' were not found to correlate well with surface inhomogeneities, such as clearings in the forest, changes in surface albedo, and changes in surface moisture. If this type of phenomenon were to be superimposed on the preexisting moisture gradient in the dryline environment, it would likely result in the steplike moisture profile found in this and other recent dryline studies.

With this in mind, it is important to examine each of the steplike changes associated with the relevant cases in this study in order to find any similarity in the sec-

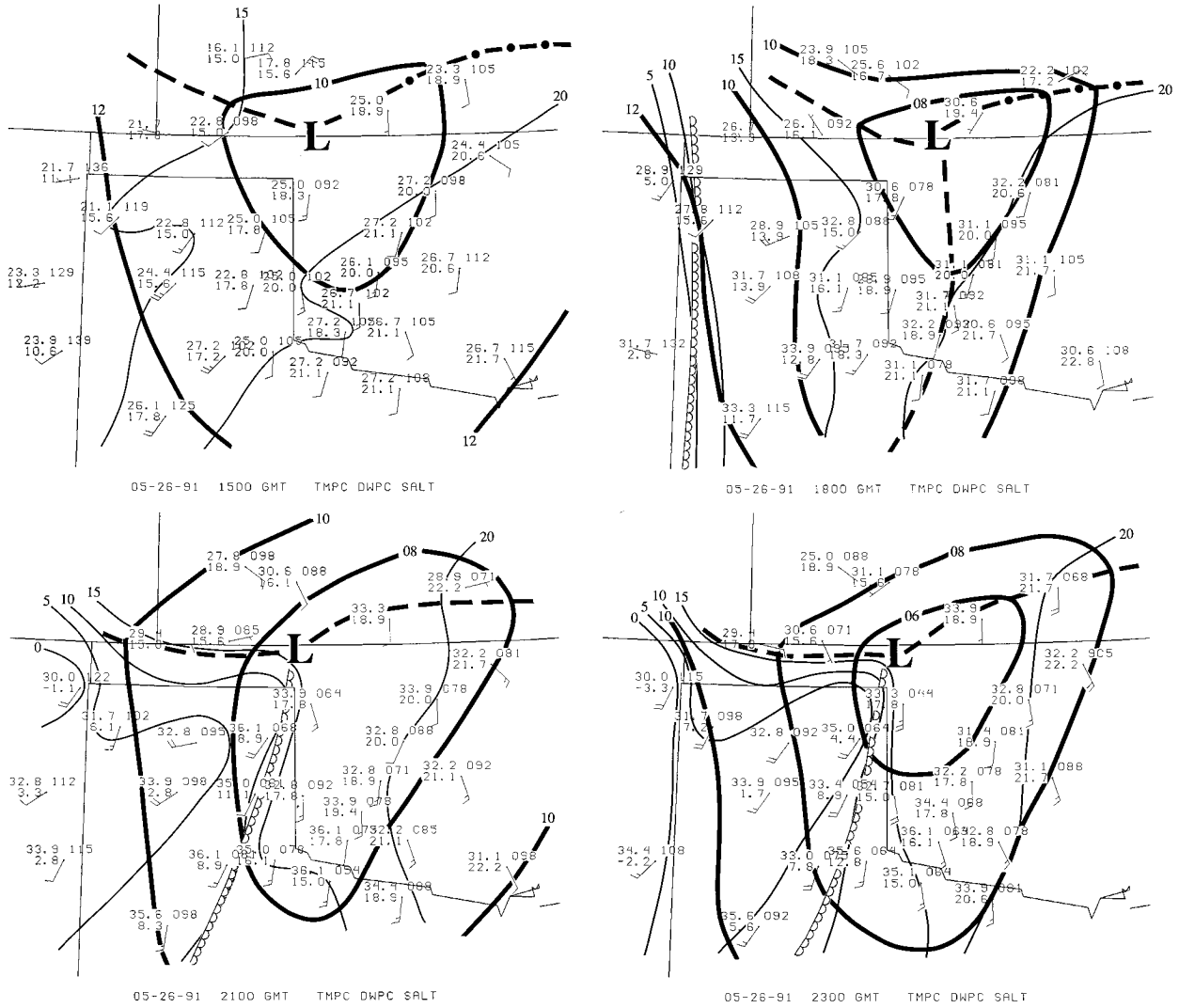

FIG. 10. As in Fig. 3 but at (a) 1500, (b) 1800, (c) 2100, and (d) 2300 UTC 26 May 1991, and without the highlighted triangle.

ondary characteristics associated with them, that is, changes in wind direction, wind speed, pressure, and temperature. At Stinnett on 30 May 1991 (Fig. 9), four steplike drops in dewpoint occurred, at approximately 1615, 1735, 2000, and 2120 UTC. No significant response is detected in either the pressure or virtual temperature field. However, as documented in section 3a, each of the steps was associated with a distinct veering of the wind. Any such correlations were not evident in either of the other two cases (Fig. 11). With the limited data and inadequate observational capabilities available, we can only speculate that the steps in the moisture field are due to periodic bursts of turbulent kinetic energy (TKE) originating from the drier air above the capping inversion east of the dryline. One of the causes of this TKE production is likely the locally enhanced wind shear due to the return branch of the secondary circulation associated with the convergence at the dryline. Shear production is responsible for the greatest amount of TKE production (in the u and v components) near the surface in the convective boundary layer (Lenschow et al. 1980). The mixing of this air with the more moist air beneath the capping inversion would explain the periodic drying and veering that occurs in the 30 May 1991 Stinnett case at least. To test these hypotheses, however, it is necessary to employ numerous fast-response observing platforms across the dryline environment for many different cases. To this date, this endeavor has not been undertaken.

There are other plausible mechanisms that may explain the stepped progression of some drylines. It might be that the dryline often advances in discrete steps as convective temperature is reached over a broad zone, rather than just along a narrow zone defining the dryline

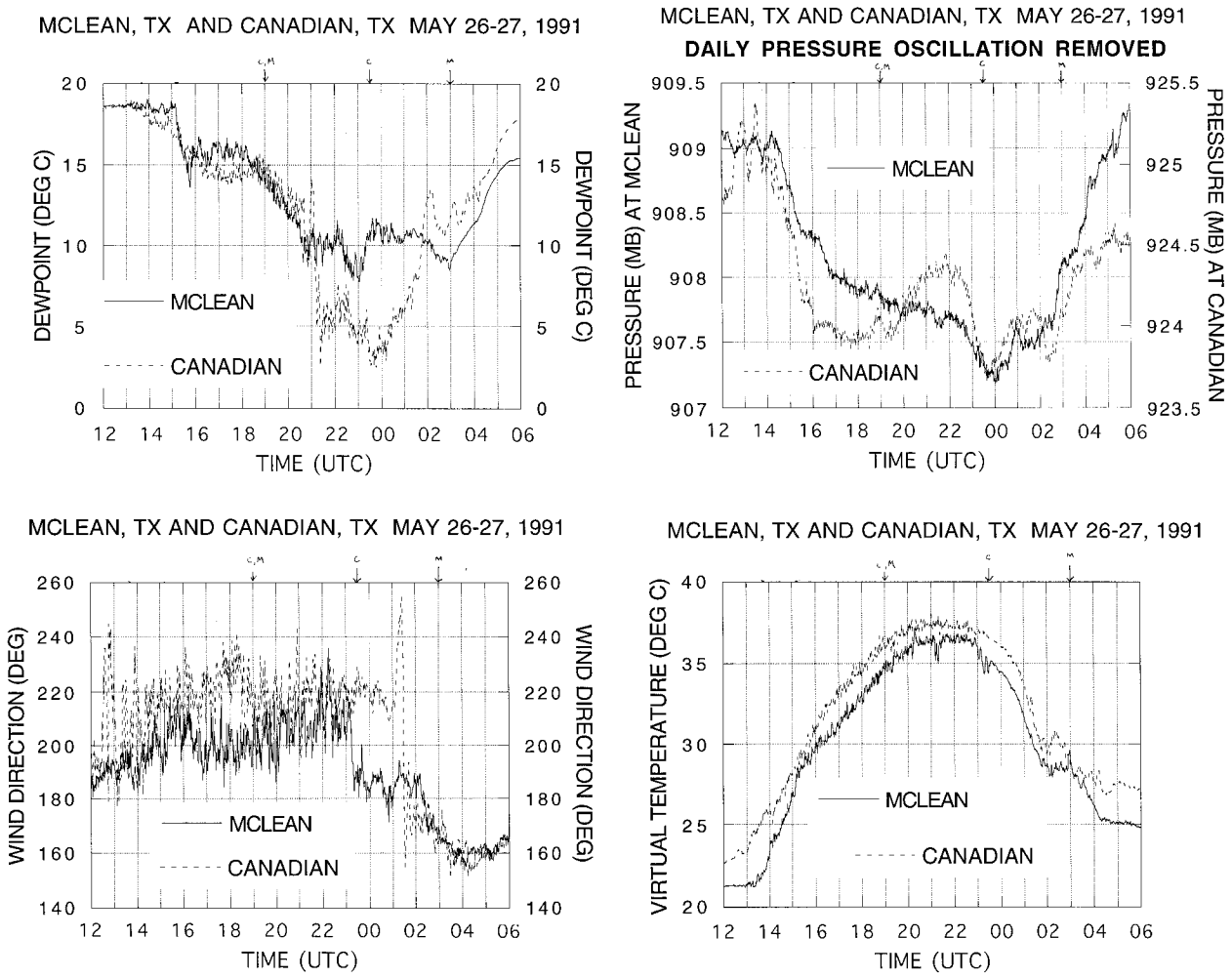

FIG. 11. Plots at McLean (solid line) and Canadian (dashed line) of (a) dewpoint, (b) adjusted pressure, (c) wind direction, and (d) virtual temperature as a function of time. First arrow at top marked ''C'' (''M'') denotes time of eastward dryline passage at Canadian (McLean); second arrow at top marked ''C'' (''M'') denotes time of westward passage at Canadian (McLean).

at that instant. Convective temperature may be attained simultaneously along a broad zone perhaps because topography on a fine scale resembles steps more than it does a uniformly sloping surface or possibly because there are steplike changes in other variables, such as soil moisture, land use, cloud cover, etc. It is interesting, though not statistically significant, that this stepped-dryline behavior commenced during the morning hours in all three of these cases. Conversely, the only distinct afternoon eastward dryline passage (30–31 May 1991, at Quitaque) was characterized by one distinct, sharp dewpoint drop. To date, the relative paucity of sample cases does not allow us to determine if stepped drylines are more commonly found earlier in the day. It may be that weaker gradients can exist when vertical turbulent mixing is relatively weak but are destroyed as the turbulent velocity fluctuations and the scale of the boundary layer eddies become larger.

5. Summary and conclusions

The character of dewpoint change across eastward-moving drylines during COPS-91 varied widely. In some instances the dewpoint dropped many degrees Celsius on a timescale of tens of minutes (Fig. 4a), while in others it dropped about the same amount on a timescale of hours (Fig. 13a). There was no correlation of the rate of dewpoint drop with the occurrence of deep cumulus convection.

In some instances there was a relative minimum in adjusted pressure along the eastward-moving dryline (Figs. 4b, 9b), while in others there was not (Figs. 11b, 13b). However, owing to the difficulty in applying time-to-space conversion to data from drylines that progress eastward in discrete steps, and to the unknown contribution from the horizontal gradient in local pressure tendency, it is not possible to make a definitive statement

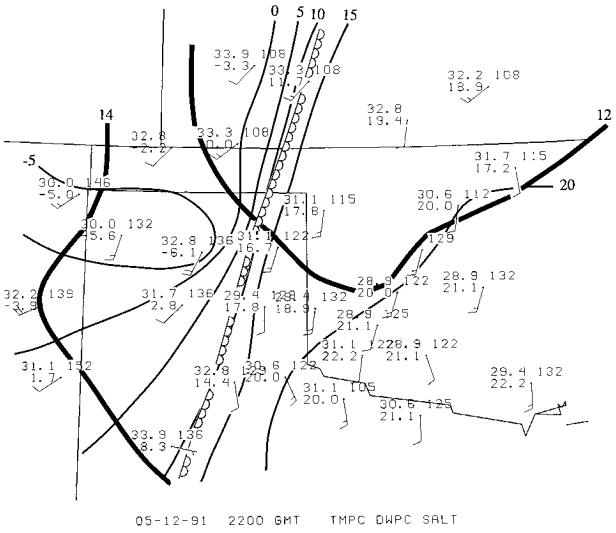

FIG. 12. As in Fig. 3 but at 2200 UTC 12 May 1991.

about whether or not the dryline is actually collocated with a pressure trough on the basis of time series alone. In the case of the sharpest dryline passage (Fig. 4b), however, there was in fact a well-defined pressure minimum at the time of dryline passage. The pressure signature may be less well defined in weaker drylines or in those that progress in discrete steps. In one case (Fig. 10) the dryline during the morning was not collocated with a pressure trough but later jumped eastward and became located near a pressure trough. From the surface analyses it is concluded that the dryline is not always collocated with a pressure trough.

Again, owing to the difficulty in applying time-to-space conversion to time series of dryline data, it is difficult to make conclusive statements about the nature of the virtual temperature gradient, if any, across eastward-moving drylines. In the case of the sharpest dryline passage (Fig. 4b), the virtual temperature did rise about 0.5°C as the dryline passed by the PAM-II site. Other well-defined changes in virtual temperature that were correlated with the eastward passage of the dryline were detected only on 26 May at McLean (Fig. 11d; just after 1500). Ziegler et al. (1994), in their numerical

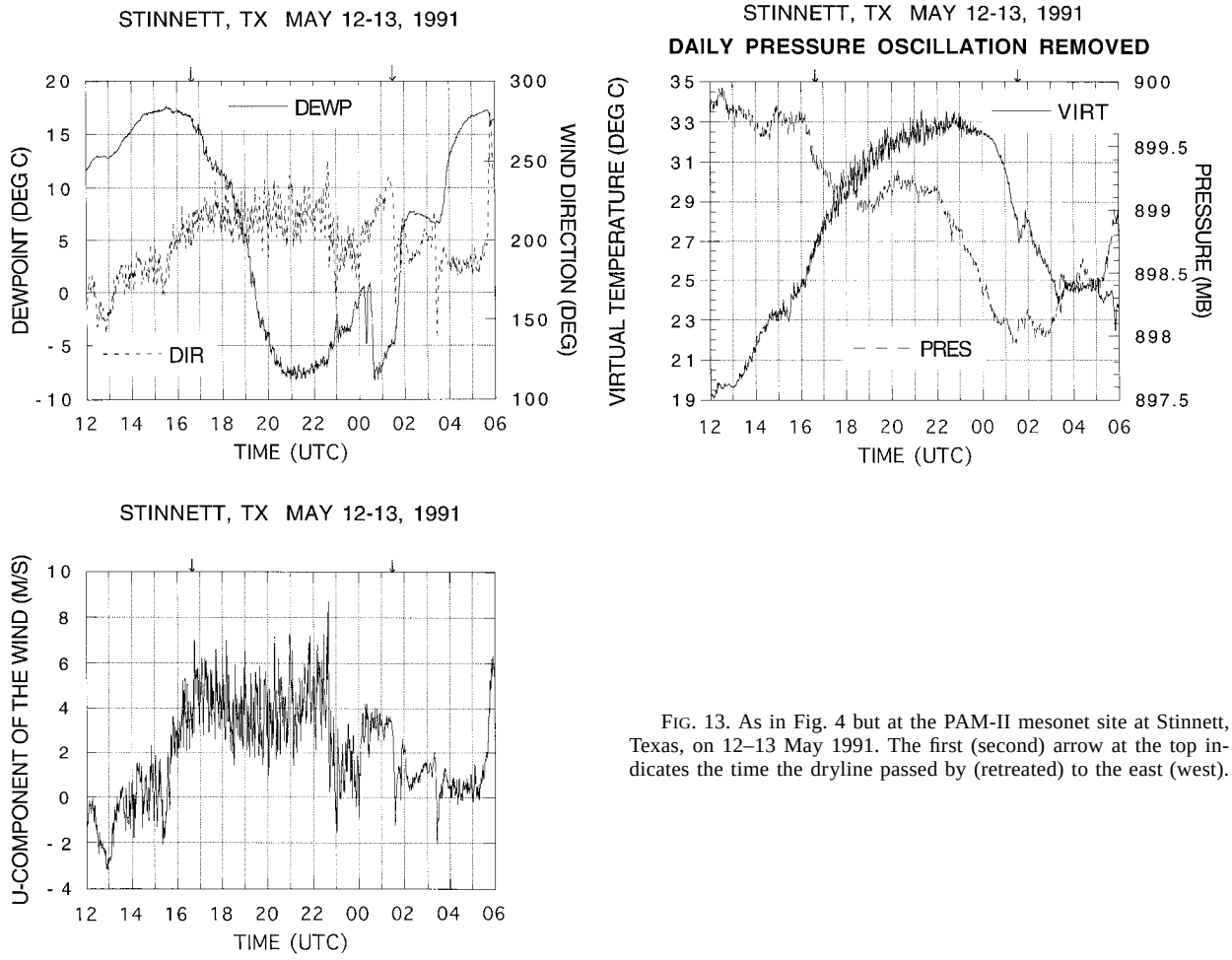

FIG. 13. As in Fig. 4 but at the PAM-II mesonet site at Stinnett, Texas, on 12–13 May 1991. The first (second) arrow at the top indicates the time the dryline passed by (retreated) to the east (west).

simulations of a dryline, noted surface virtual temperature differences across the dryline late in the afternoon that were slightly larger than 0.5°–1°C; however, the virtual temperature differences had been much weaker earlier in the day. During COPS-91 most of the virtual temperature traces representing dryline passage before midafternoon did not reveal any significant increase other than a diurnal rise.

Westward-moving drylines during COPS-91 did not behave like a classic thunderstorm gust-front density current (Goff 1976) since there was no detectable pressure jump when the dryline had passed by. Density currents are driven by the hydrostatic pressure gradient across them (Benjamin 1968). The virtual temperature drops observed on the order of 1°C or less were not enough to change the surface pressure noticeably. It is possible that the initial westward surge of moisture was so shallow that the hydrostatic pressure was unaffected. One would expect that the greatest cross-dryline difference in virtual temperature would occur during the late afternoon, when the cross-dryline temperature gradient is strongest. In some cases, low overcast is prevalent east of the dryline throughout the day. Perhaps the dryline is most similar to a density current in these situations, when the cross-dryline temperature gradient would be particularly strong. The main point is that a westward-moving dryline passage does not always result in significant, simultaneous changes in dewpoint, wind, and pressure, as the ''density current theory'' would imply. The increased temporal and spatial resolution afforded by the use of the PAM-II stations has been utilized to show that *many drylines do not fit nicely into the current conceptual models,* which are based mainly on numerical simulations of ''classic'' drylines.

The period of oscillations in dewpoint and wind direction west of the dryline in the 30–31 May case is too short (90 min) to be associated with an inertial wave (which at 34°N is approximately 200 min, more than twice as long). In the upper troposphere north of Midland, the absolute vorticity was relatively low, owing to anticyclonic shear (Fig. 7). Inertial instability, however, probably did not play a role because the absolute vorticity was not negative. Oscillations in wind and dewpoint such as those documented do not appear to be a feature characteristic of the dryline but rather one linked to external conditions. Circumstantial evidence from water vapor imagery suggested that the waves may have been associated with a disturbance aloft. Koch (1979) has argued that evanescent gravity waves may propagate downward into the boundary layer and surface layer in spite of a neutral or unstable stratification as is found west of the dryline. Since no oscillations in the surface pressure were detected, the surface oscillations were not gravity waves. Suppose, however, that the oscillations were a result of the periodic mixing down of relatively high zonal momentum (McCarthy and Koch 1982) associated with gravity wave motion in the middle or upper troposphere. The diagnostic pressure equation relating the pressure field to horizontal variations in turbulent mixing is as follows (cf. Bluestein 1992, 276):

$$\nabla_z^2 p = \frac{\partial}{\partial x}(\rho F_x) + \frac{\partial}{\partial y}(\rho F_y), \tag{1}$$

where F_x and F_y are the x and y components of $\mathbf{F}_Z$, which is the ''turbulent friction'' term in the horizontal equations of motion. Specifically, $\mathbf{F}_Z$ represents the acceleration due to turbulent vertical mixing of horizontal momentum. The magnitude of pressure oscillations associated with variations in turbulent mixing on a horizontal scale of L is on the order of $\rho LF_x \approx \rho Lu'w'/H$, where u' and w' represent the scale of turbulent eddies in u and w, and H is the vertical scale. For L, H, u', and w' of 50 km (cf. Fig. 5), 5 km (depth of air column extending from the ground up to the middle portion of the troposphere), 5 m s^{-1} (cf. Fig. 4c), and 50 cm s^{-1} ($w' \approx u'H/L$), the amplitude of pressure oscillations is only on the order of 0.25 mb, which is below the threshold of instrument observing error. Thus, if the oscillations in surface wind were due to the periodic mixing down of higher momentum, it would be difficult or impossible to detect corresponding surface pressure oscillations in this particular case.

This study made use of a modest network of mesonet sites. Since COPS-91 was conducted, a denser, *operational* network of over 100 mesonet stations has been installed in Oklahoma (The Oklahoma Mesonet; Brock et al. 1995). With this network, higher resolution (in both space and time) studies are possible.

Acknowledgments. This study was funded by NSF research Grants ATM-9019821 and ATM-9302379. The Surface and Sounding Systems Facility of ATD at NCAR provided the PAM-II stations with partial support from NASA coutesy of Steve Koch. Some of this research was done while the second author was a summer visitor at the MMM Division of NCAR. The NCAR Graphics group assisted with most of the figures. NCAR is funded by the National Science Foundation. Sue Weygandt at OU/CAPS also assisted with some of the figures. We are indebted to personnel at NSSL for providing the PAM-II site surveys. Irv Watson (NSSL) provided some data not available in the OU archive. Fred Carr (OU), Bob Davies-Jones (NSSL), Carl Hane (NSSL), Conrad Ziegler (NSSL), and Mark Morrissey (OU) provided helpful advice.

REFERENCES

André, J. C., J. P. Goutorbe, and A. Perrier, 1986: HAPEX-MOBILHY: A hydrologic atmospheric experiment for the study of water budget and evaporation flux at the climatic scale. *Bull. Amer. Meteor. Soc.,* **67,** 138–144.

Beebe, R. G., 1958: An instability line development as observed by the tornado research airplane. *J. Atmos. Sci.,* **15,** 278–282.

Benjamin, T. B., 1968: Gravity currents and related phenomena. *J. Fluid Mech.,* **31,** 209–248.

Betts, A. K., 1982: Saturation point analysis of moist convective overturning. *J. Atmos. Sci.,* **39,** 1484–1505.

Bluestein, H. B., 1992: *Synoptic–Dynamic Meteorology in Midlatitudes.* Vol. I, *Principles of Kinematics and Dynamics,* Oxford University Press, 431 pp.

——, and S. Parker, 1993: Modes of isolated, severe convective-storm formation along the dryline. *Mon. Wea. Rev.,* **121,** 1354–1372.

——, E. W. McCaul Jr., G. P. Byrd, and G. R. Woodall, 1988: Mobile sounding observations of a tornadic storm near the dryline: The Canadian, Texas storm of 7 May 1986. *Mon. Wea. Rev.,* **116,** 1790–1804.

——, ——, ——, ——, G. Martin, and S. Keighton, 1989: Mobile sounding observations of a thunderstorm near the dryline: The Gruver, Texas storm complex of 25 May 1987. *Mon. Wea. Rev.,* **117,** 244–250.

Brock, F. V., G. H. Saum, and S. R. Semmer, 1986: Portable Automated Mesonet II. *J. Atmos. Oceanic Technol.,* **3,** 573–582.

——, K. C. Crawford, R. L. Elliot, G. W. Cuperus, S. J. Stadler, H. L. Johnson, and M. D. Eilts, 1995: The Oklahoma Mesonet: A technical overview. *J. Atmos. Oceanic Technol.,* **12,** 5–19.

Chapman, S., and R. S. Lindzen, 1970: *Atmospheric Tides.* D. Riedel, 200 pp.

Davies-Jones, R., and D. P. Zacharias, 1988: Contributing factors in the 10 May 1985 tornado outbreak in northwest Kansas. Preprints, *15th Conf. on Severe Local Storms,* Baltimore, MD, Amer. Meteor. Soc., 284–287.

Dowell, D. C., H. B. Bluestein, and D. P. Jorgensen, 1997: Airborne Doppler radar analysis of supercells during COPS-91. *Mon. Wea. Rev.,* **125,** 365–383.

Fujita, T. T., 1958: Structure and movement of a dry front. *Bull. Amer. Meteor. Soc.,* **39,** 574–582.

——, 1970: The Lubbock tornadoes: A study of suction spots. *Weatherwise,* **23,** 160–173.

Goff, R. C., 1976: Vertical structure of thunderstorm outflows. *Mon. Wea. Rev.,* **104,** 1429–1440.

Hane, C. E., C. L. Ziegler, and H. B. Bluestein, 1993: Investigation of the dryline and convective storms initiated along the dryline: Field experiments during COPS-91. *Bull. Amer. Meteor. Soc.,* **74,** 2133–2145.

——, H. B. Bluestein, T. M. Crawford, M. E. Baldwin, and R. M. Rabin, 1997: Severe thunderstorm development in relation to along-dryline variability: A case study. *Mon. Wea. Rev.,* **125,** 231–251.

Haurwitz, B., 1955: The thermal influence on the daily pressure wave. *Bull. Amer. Meteor. Soc.,* **36,** 311–317.

Koch, S. E., 1979: Mesoscale gravity waves as a possible trigger of severe covection along a dryline. Ph. D. dissertation, University of Oklahoma, 195 pp. [Available from School of Meteorology, University of Oklahoma, 100 East Boyd, Room 1310, Norman, OK 73019-0470.]

——, and J. McCarthy, 1982: The evolution of an Oklahoma dryline. Part II: Boundary-layer forcing of mesoconvective systems. *J. Atmos. Sci.,* **39,** 237–257.

Lenschow, D. H., J. C. Wyngaard, and W. T. Pennel, 1980: Mean-field and second-moment budgets in a baroclinic convective boundary layer. *J. Atmos. Sci.,* **37,** 1313–1326.

Mahrt, L., 1991: Boundary layer moisture regimes. *Quart. J. Roy. Meteor. Soc.,* **117,** 151–176.

McCarthy, J., and S. E. Koch, 1982: The evolution of an Oklahoma dryline. Part I: Meso- and subsynoptic-scale analysis. *J. Atmos. Sci.,* **39,** 225–236.

McGuire, E. L., 1960: The vertical structure of three drylines as revealed by aircraft traverses. National Severe Storms Project Rep. 7, 11 pp. [Available from School of Meteorology, University of Oklahoma, 100 East Boyd, Room 1310, Norman, OK 73019-0470.]

NSSP Staff, 1963: Environmental and thunderstorm structures as shown by National Severe Storms Project observations in spring 1960 and 1961. *Mon. Wea. Rev.,* **91,** 271–292.

Parsons, D. B., M. A. Shapiro, R. M. Hardesty, R. J. Zamora, and J. M. Intrieri, 1991: The finescale structure of a west Texas dryline. *Mon. Wea. Rev.,* **119,** 1283–1292.

Rhea, J. O., 1966: A study of thunderstorm formation along dry lines. *J. Appl. Meteor.,* **5,** 58–63.

Sanders, F., and D. O. Blanchard, 1993: The origin of a severe thunderstorm in Kansas on 10 May 1985. *Mon. Wea. Rev.,* **121,** 133–149.

Schaefer, J. T., 1974a: The life cycle of the dryline. *J. Appl. Meteor.,* **13,** 444–449.

——, 1974b: A simulative model of dryline motion. *J. Atmos. Sci.,* **31,** 956–964.

Shaw, B. L., R. A. Pielke, and C. L. Ziegler, 1997: The effect of soil moisture heterogeneity on a Great Plains dryline: A numerical study. *Mon. Wea. Rev.,* in press.

Simpson, G. C., 1918: The twelve-hourly barometer oscillation. *Quart. J. Roy. Meteor. Soc.,* **44,** 1–18.

Simpson, J. E., 1969: A comparison between laboratory and atmospheric density currents. *Quart. J. Roy. Meteor. Soc.,* **95,** 758–765.

Sun, W.-Y., and C.-C. Wu, 1992: Formation and diurnal variation of the dryline. *J. Atmos. Sci.,* **49,** 1606–1619.

United States Department of Commerce, 1943: Ten-year normals of pressure tendencies and hourly station pressures for the United States. U. S. Weather Bureau Tech. Paper 1, 63 pp. [Available from School of Meteorology, University of Oklahoma, 100 East Boyd, Room 1310, Norman, OK 73019-0470.]

Ziegler, C. L., and C. E. Hane, 1993: An observational study of the dryline. *Mon. Wea. Rev.,* **121,** 1134–1151.

——, T. J. Lee, and R. A. Pielke, 1994: Simulations of the dryline with a 3-D mesoscale model. Preprints, *Sixth Conf. on Mesoscale Processes,* Portland, OR, Amer. Meteor. Soc., 242–245.

——, W. J. Martin, R. A. Pielke, and R. L. Walko, 1995: A modeling study of the dryline. *J. Atmos. Sci.,* **52,** 263–285.